

Characterization, Electrical and Magnetic properties of light rare earth Zirconate

POOJARAGHUVANSHI and A.N. THAKUR

Department of Physics, T.D. Post Graduate College Jaunpur-222002 U.P. (INDIA)
Email :- ant_tdc@yahoo.com, poojaraghuvanshi@yahoo.com

(Acceptance Date 4th April, 2012)

Abstract

The $\text{Pr}_2\text{Zr}_2\text{O}_7$ compound is prepared by using solid state reaction technique. Its structural, electrical and magnetic properties have been investigated. X-ray diffraction pattern indicates that $\text{Pr}_2\text{Zr}_2\text{O}_7$ crystallizes in an orthorhombic perovskite structure. The compound was characterized through powder differential thermal analysis (DTA), thermogravimetric analysis (TGA) and derivative thermogravimetry (DTG). The electrical conductivity (σ), dielectric constant (ϵ'), dielectric loss (ϵ'') and quality factor (Q) of $\text{Pr}_2\text{Zr}_2\text{O}_7$ was measured in the temperature range 300-1125K at an internal frequency of 1kHz. . The $\log \sigma$ vs $10^3/T$ plot yield two different slopes separated by break temperature (T_I). The activation energy below and above T_I have been estimated as 0.10eV and 2.7eV respectively. Hence the electrical conductivity below T_I is essentially extrinsic always associated with impurities, defects and interstitials and conductivity above T_I is essentially intrinsic due to the change in conduction mechanism. The magnetic susceptibility of the compound was measured in the temperature range 300-1100K at field 1.55×10^{-1} Tesla. The magnetism in this compound arises from the rare-earth ions, while Zr is non magnetic.

Key words: XRD, DTA, TGA, DTG, $\text{Pr}_2\text{Zr}_2\text{O}_7$

1. Introduction

The lanthanide zirconate pyrochlores ($\text{Ln}_2\text{Zr}_2\text{O}_7$) with pyrochlore structure has complex chemistry, low thermal conductivity high thermal expansion coefficient and high

chemical stability behaviours, which are considered to have wide applications, such as nuclear applications, sub-catalysts for automotive exhaust gases, high temperature thermal-barrier coating materials, hosts for fluorescence centres and oxidation catalysis. Zirconates are

very interesting compounds from many scientific and technological points of view because of their electronic and magnetic properties. They have a broad range of applications as high temperature heating elements, oxidation catalyst, fuel cells, oxygen sensors and thermal barrier^{1,2}. The electrical properties of these material make them promising candidates for fuel cell application where high ionic conductivity and low activation energy are desired^{3,4}. The dielectric studies are informative in the study of ferroelectricity and phase transition⁵.

In this paper, we discussed the synthesis, characterization, electrical and magnetic properties of $\text{Pr}_2\text{Zr}_2\text{O}_7$ compound. The literature survey showed that only limited studies are related with their synthesis, nanoscopic characterization, spin freezing, preparation and thermal barrier coating⁶⁻⁹.

2. Experimental

2.1 Sample preparation and Characterization:

Powdered sample of $\text{Pr}_2\text{Zr}_2\text{O}_7$ was synthesized by means of a solid state using Pr_2O_7 (99.99% Alfa Aesar) and ZrO_2 (99.7% Alfa Aesar). The stoichiometric amounts of Pr_2O_7 and ZrO_2 were thoroughly mixed in an agate mortar for 3 hrs in wet medium and then dried and calcined in alumina crucible at 1300K for 50 hrs in air atmosphere followed by one intermediate grinding. The final product was cool down slowly.

The powdered sample was characterised by means of an X-ray diffractometer (Thermoelectron - XRL EXTRA) at room

temperature using $\text{CuK}\alpha$ radiation with $\lambda=0.15418\text{nm}$ in wide range of Bragg angle ($10^\circ \leq \theta \leq 90^\circ$).

The thermal behaviour of $\text{Pr}_2\text{Zr}_2\text{O}_7$ was studied from 323K to 1123K using differential thermal analysis (DTA), thermogravimetric analysis (TGA) and differential thermal analysis (DTG) (PERKIN ELEMER PYRIS). The experiments were conducted in nitrogen gas at a heating rate of 283K/min and flow rate of 100ml/min.

2.2 Electrical Conductivity Measurement:

The electrical conductivity of sample was measured by finding out the resistance of the sample on pressed pellet by two electrode method. The pellet (Area $\sim 0.95 \times 10^{-4} \text{m}^2$ and thickness $\sim 0.30 \times 10^{-2} \text{m}$) was prepared from homogenous powder of $\text{Pr}_2\text{Zr}_2\text{O}_7$ at isostatic pressure at $7.19 \times 10^8 \text{Nm}^{-2}$ using hydraulic press. The pellet was then sintered at 1500K in air atmosphere for 30hrs. Both the faces of the sintered sample were coated with high purity air drying silver paint after making both surfaces flat and parallel and then inserted between two silver electrodes. The silver foils were electrically insulated from the sample holders by mica sheets. The electrical conductivity was measured by an autocompute LCR-Q meter (Model 928, Systronics India).

2.3 Dielectric measurement :

An autocompute LCR-Q meter (model 928, Systronics India) was used to measure the capacitance (c) and quality factor (Q) of the sample at different temperature and at a frequency of 1kHz. The dielectric constant

(ϵ') and dielectric loss (ϵ'') of the sample was calculated by using the following relation^{10,11}

$$\epsilon' = \frac{ct}{\epsilon_0 A} \quad (1)$$

$$\epsilon'' = \frac{\epsilon'}{Q} \quad (2)$$

Where c = the capacitance of the capacitor in Farad, t = the thickness, A = face area of the pallet, ϵ_0 = permittivity of free space and Q = quality factor respectively.

2.4 Magnetic Measurement :

Magnetic susceptibility measurements were done on powdered sample using Faraday's method^{12,13}. $Gd_2(WO_4)_3$ has been used for standardization.

3 Result and Discussion

Figure 1 shows the XRD pattern of $Pr_2Zr_2O_7$. From XRD pattern, d_{hkl} values have been obtained using the relation¹⁴.

$$d_{hkl} = \frac{0.15418}{2\sin\theta} \quad (3)$$

From these values of d_{hkl} , structure of the studied compounds was resolved using usual procedure. All the peaks have been assigned with proper hkl values. This confirms that prepared compounds has single phase and no unreacted part of the material was left. The unit cell is orthorhombic and the lattice constant was estimated to be $a_0=2.5614$, $b_0=1.6740$ nm and $c_0=1.4295$ nm.

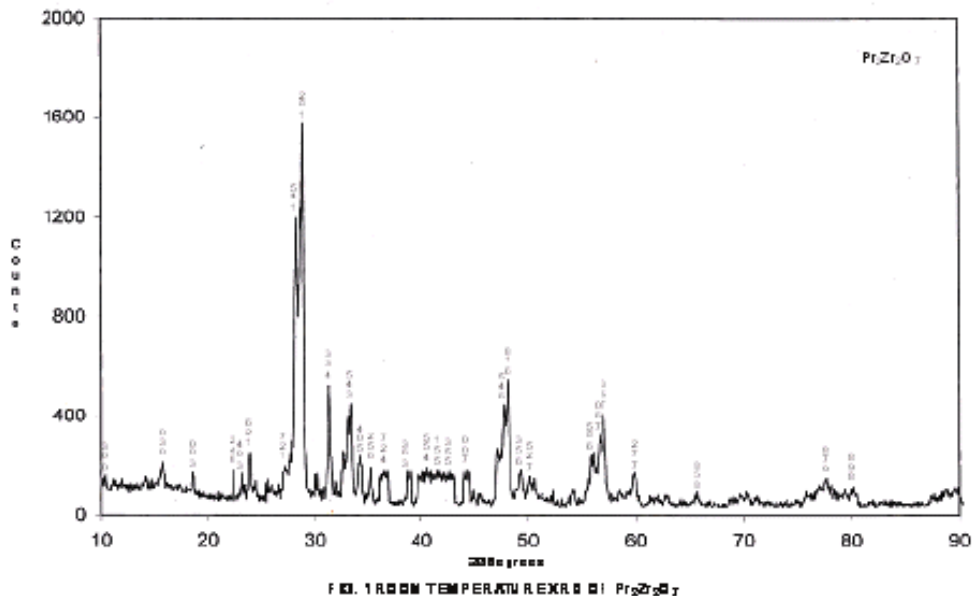


Fig. 1. Room temperature xrd of $Pr_2Zr_2O_7$

Figure 2 presents the DTA, TGA and DTG trace of $\text{Pr}_2\text{Zr}_2\text{O}_7$. DTA trace show endothermic peaks at 558K. The corresponding TGA trace shows weight loss in two successive steps. The first step of weight loss 0.25% is from 323K to 523K may be due to removal of absorbed

water and other gaseous species. The second step of weight loss 1.5% is from 523K to 648K and above 648K the compound is stable. The DTG trace show maximum rate of mass change at 558K.

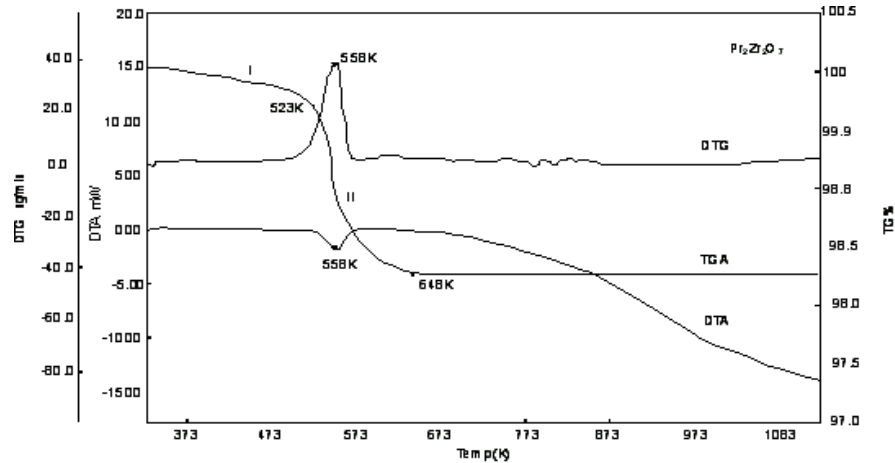


FIG 2 TGA, DTA AND DTG CURVE OF $\text{Pr}_2\text{Zr}_2\text{O}_7$

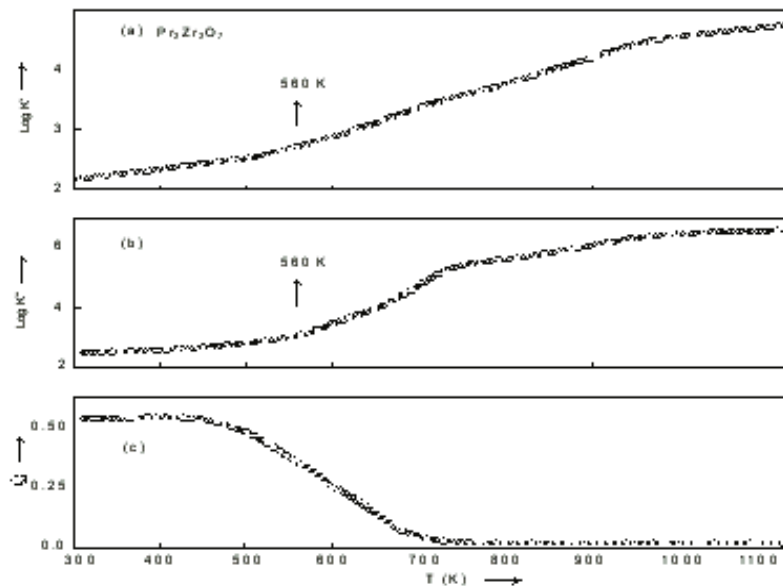


FIG. 3 (a) PLOTS OF LOGARITHM OF DIELECTRIC CONSTANT ($\text{Log } K$) AGAINST ABSOLUTE TEMPERATURE (T)
 (b) PLOTS OF LOGARITHM OF DIELECTRIC LOSS ($\text{Log } K'$) AGAINST ABSOLUTE TEMPERATURE (T)
 (c) PLOTS OF QUALITY FACTOR (Q) AGAINST ABSOLUTE TEMPERATURE (T)

Figure 3. Shows the variation of dielectric constant (ϵ'), dielectric loss (ϵ'') and quality factor with temperature at 1kHz. The dielectric constant of $\text{Pr}_2\text{Zr}_2\text{O}_7$ at 400K is 211. At lower temperature the dielectric constant (ϵ') seems to have almost no temperature dependence, so these values may be taken as the room temperature values of the materials. The reported values of ϵ' has been calculated using the capacitance value for the pellet. The density of this pellet remains less than the theoretical density of this material. This means pellets contain air pores. Therefore a correction for pore fraction (f_p) is essential to obtain the bulk value of the dielectric constant (ϵ'_b) and is given by relation¹⁵.

$$f_p = \frac{d_0 - d_p}{d_0} \quad (4)$$

The theoretical density (d_0), pellet density (d_p) and pore fraction of $\text{Pr}_2\text{Zr}_2\text{O}_7$ are $3.68 \times 10^3 \text{ Kg m}^{-3}$, $3.67 \times 10^3 \text{ Kg m}^{-3}$ and $f_p = 0.003$ respectively. For low conducting solid, ϵ'_b , ϵ' , and f_p are related by the relation¹⁶.

$$\epsilon'_b = \frac{(\epsilon'^{1/3} - f_p)^3}{1 - f_p} \quad (5)$$

The evaluated values of ϵ'_b is 211.

The values of ϵ' become large as temperature is increased and validity of eqⁿ (5) becomes doubtful. Further this formula affects only the magnitude but not the nature of temperature variation of ϵ' . Therefore we have not used this correction at higher temperatures. The values of dielectric constant (ϵ') and dielectric loss (ϵ'') at temperature 400k, 600K, 800K and 1000K at frequency

1kHz are given in table 1 and 2 respectively.

Table 1. Dielectric constant (ϵ') of $\text{Pr}_2\text{Zr}_2\text{O}_7$ at different temperature.

Compound	400K	600K	800K	1000K
$\text{Pr}_2\text{Zr}_2\text{O}_7$	211	446.68	5.62×10^2	3.55×10^3

Table 2. Dielectric loss (ϵ'') of $\text{Pr}_2\text{Zr}_2\text{O}_7$ at different temperature.

Compound	400K	600K	800K	1000K
$\text{Pr}_2\text{Zr}_2\text{O}_7$	446.68	3548.13	2.8×10^5	2.8×10^6

The dielectric constant has very slow increase at lower temperature. This shows that there is no chance for the existence of thermally generated charge carrier at lower side of temperature. Well made electrode rules out the possibility of interfacial polarization. Therefore this slow increase seems to be the combined effect of lattice and electronic polarizability of individual ions. The increase of these polarizabilities seems to compensate the slight decrease of polarizability due to decrease in the number of ions per unit volume following the lattice expansion with temperature. However it must be noticed that the increase of ϵ' with T is very slow in comparison to the variation one expects for ionic solids. This indicates that either thermal expansion of these materials is very small or they have some other kind of polarization mechanism.

The dielectric constant (ϵ') has much faster increase above certain critical temperature ($T_k = 560\text{K}$). The dielectric loss (ϵ'') shows similar behaviour above T_k .

The rapid increase in dielectric constant above T_k is due to space charge polarization^{17,18}.

The pressed sample develops a considerable amount of space charge polarization arising out from the defects or impurities present in the bulk or at the surface of the material.

The electrical conductivity (σ) have been measured in the temperature range 300-1125K at frequency 1kHz. The variation of $\text{Log}\sigma$ vs $10^3/T$ is shown in Fig. 4. The curve follows the well known exponential relation for

semiconductor $\sigma = \sigma_0 \exp(-E_a/kT)$ but with two different slopes. A kink occurs at T_1 ($T_1 = 550\text{K}$) termed as break temperature. The pre-exponential constant (σ_0) and activation energy (E_a) have been calculated from the slopes. The values of pre exponential constant, activation energy and break temperature have been presented in table 3.

Table 3. Electrical transport parameter of $\text{Pr}_2\text{Zr}_2\text{O}_7$ compound.

Compound	Break temperature T_1	For $T < T_1$		For $T > T_1$	
		σ_0 ($\Omega^{-1}\text{m}^{-1}$)	E_a (eV)	σ_0 ($\Omega^{-1}\text{m}^{-1}$)	E_a (eV)
$\text{Pr}_2\text{Zr}_2\text{O}_7$	550	72.9×10^{-5}	0.12	2.18×10^{16}	2.6

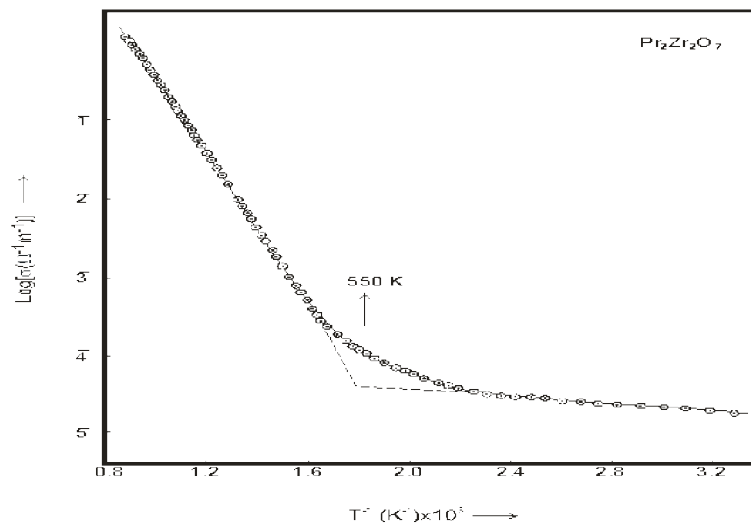


FIG. 4. PLOTS OF LOGARITHM OF ELECTRICAL CONDUCTIVITY ($\text{LOG}\sigma$) AGAINST INVERSE OF ABSOLUTE TEMPERATURE (T^{-1})

The electrical conductivity of $\text{Pr}_2\text{Zr}_2\text{O}_7$ at room temperature is $\sigma = 10^{-4} \Omega^{-1}\text{m}^{-1}$ which indicate that the compound is insulator. However with increasing temperature their conductivity rapidly increases and becomes conductor.

The activation energies below and above break temperature are nearly 0.12eV and 2.6eV respectively. In semiconducting materials, the electrical conduction at low temperature is always associated with

impurities, defects and interstitials which generally provide states in forbidden energy gap of the material and lower value of activation energy. The contribution of defects or impurities towards conduction in solid can be explained in terms of donors or acceptors and is represented by expression¹⁹.

$$\sigma_d = A \exp\left(\frac{-E_i}{KT}\right) \quad (6)$$

Where E_i is ionization energy of donors or acceptors and usually $E_i \sim 0.12\text{eV}$ for semiconducting material. The activation energy below break temperature is found approximately comparable to the ionization energy E_i and therefore the conclusion is that electrical conduction is certainly due to impurities, point

defects, or interstitials seems to be reasonable.

The activation energy $\sim 2.6\text{eV}$ estimated in the higher temperature range $T > T_1$ seems to be an intrinsic because σ_0 is in the correct range for intrinsic conductivity. Thus the change in the nature of the $\log\sigma$ vs $10^3/T$ curve at T_1 is due to the change in the conduction mechanism *i.e.* transition from extrinsic to intrinsic conduction.

The magnetic susceptibility measurement of $\text{Pr}_2\text{Zr}_2\text{O}_7$ was done in heating and cooling cycles. No hysteresis was observed and χ_M values were found to be same in heating and cooling cycles, although a small loss of weight is detected in heating cycle may be due to presence of moisture. The results are shown in Fig. (5) as χ_M^{-1} vs T plots. At higher

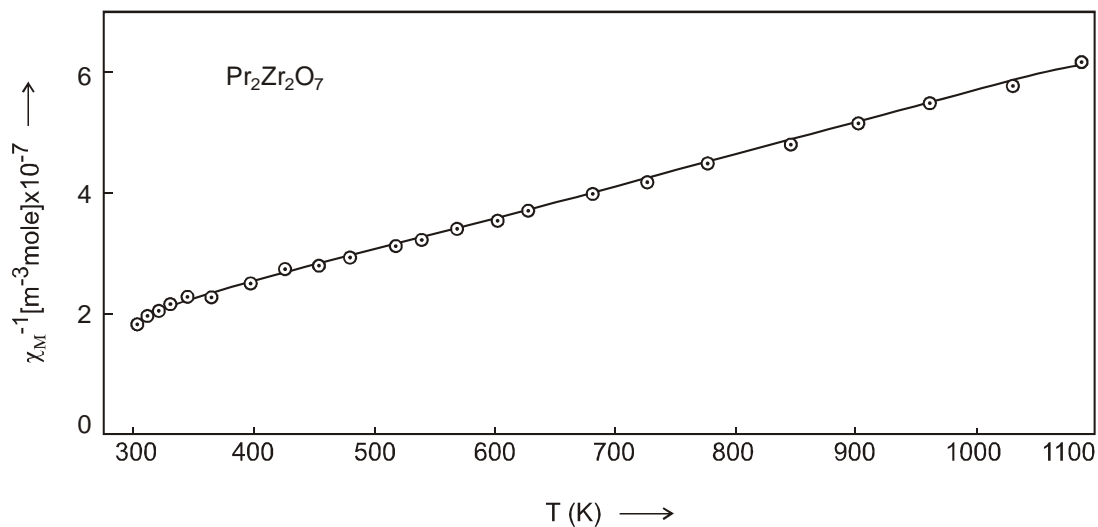


Fig. 5 VARIATION OF INVERSE OF MOLAR MAGNETIC SUSCEPTIBILITY (χ_M^{-1}) WITH ABSOLUTE TEMPERATURE OF $\text{Pr}_2\text{Zr}_2\text{O}_7$

temperature the χ_M^{-1} vs T plots are linear and obey Curie-Weiss law¹⁸.

$$\chi_M^{-1} = \frac{T - \theta_p}{\bar{C}_M} \quad (7)$$

Where θ_p is paramagnetic Curie temperature and \bar{C}_M is the molar Curie constant.

$\text{Pr}_2\text{Zr}_2\text{O}_7$ is magnetically simple because magnetism arises from the trivalent rare earth ions *i.e.* the magnetic interaction exists in $\text{Pr}_2\text{Zr}_2\text{O}_7$ is $\text{R}^{+3} - \text{R}^{+3}$ (R-rare-earth ions). Thus at temperature much higher than ordering temperature the molar magnetic susceptibility of $\text{Pr}_2\text{Zr}_2\text{O}_7$ can be approximated by the relation²⁰.

$$\chi_M = \frac{N\mu_0\mu_\beta^2}{3k} \left[\frac{\bar{P}^2}{T - \theta_p} \right] \quad (8)$$

Where N is Avagadro number, μ_B is Bohr magneton, μ_0 is permeability constant, k is Boltzmann constant, \bar{P} magneton numbers of magnetic ions R^{3+} and θ_p is the paramagnetic Curie temperature. The eqn (8) can also be written as

$$\chi_M^{-1} = \frac{3k(T - \theta_p)}{N\mu_0\mu_\beta^2\bar{P}^2} \quad (9)$$

Comparing eqⁿ (7) & (9) we have

$$\bar{C}_M = \frac{N\mu_0\mu_\beta^2\bar{P}^2}{3k}$$

$$\text{or } \bar{P} = \left[\frac{3k\bar{C}_M}{N\mu_0\mu_\beta^2} \right]^{1/2} \quad (10)$$

The experimental value of \bar{P} can be evaluated from the value of \bar{C}_M obtained from χ_M^{-1} vs T plot. The theoretical value of \bar{P} has been already known. The theoretical and experimental values of \bar{P} with magnetic ions are given in Table 4 and the values of θ_p and \bar{C}_M are given Table 5.

Table 4. Magnetic ion with theoretical and experimental value of average magneton number \bar{P} of the studied compound.

Com-pounds	Magnetic ion	Theoretical value	Experimental value
$\text{Pr}_2\text{Zr}_2\text{O}_7$	Pr^{3+}	2.54	2.49

Table 5. Paramagnetic Curie temperature (θ_p) and molar Curie constant (\bar{C}_M) of the studied compound

Compounds	θ_p (K)	$\bar{C}_M \times 10^5$ ($\text{m}^3 \text{K mole}^{-1}$)
$\text{Pr}_2\text{Zr}_2\text{O}_7$	-38	0.97

It is seen from the table that there is a good agreement between theoretical and experimental values of \bar{P} , which shows that ionic moment involved in the magnetization process concern the tripositive rare earth ions.

The value of θ_p is negative for studied

compounds suggesting a possible antiferromagnetic ordering of this compound at lower temperature. However, such small values of θ_p can also be due purely to the crystal field effect with a little contribution from simple dipole-dipole interaction between the magnetic ions.

4. Conclusions

The powder XRD pattern shows the pyrochlore phase of $\text{Pr}_2\text{Zr}_2\text{O}_7$. DTA, TGA and DTG studies show that the compound is stable above certain temperature. The dielectric constant (ϵ') and dielectric loss (ϵ'') have very slow increase upto T_k . above T_k this increase becomes much faster. The reason for faster increase of ϵ' and ϵ'' above T_k is due to space charge polarization. The electrical conductivity of $\text{Pr}_2\text{Zr}_2\text{O}_7$ at room temperature is $10^{-4}\Omega^{-1}\text{m}^{-1}$ which indicates that compound is insulator. However with increasing temperature their conductivity rapidly increases and becomes conductor. Our results reveal that $\text{Pr}_2\text{Zr}_2\text{O}_7$ is a new pyrochlore antiferromagnet.

Acknowledgement

The authors are grateful to Prof. K. Das and Mr. N. K. Das, Central Research facility IIT Kharagpur for providing DTA, TGA and DTG facility and Mr. U.S.Singh, IIT Kanpur for providing XRD facility.

Reference

1. M. A. Subramanian, G. Aravamundan and G. V. Subbarao, Oxide Pyrochlore- a

review, *Prog. Solid. State Chem.* 15, 55-143 (1983).

2. S.J. Korf, H.J.A. Koopmass, B.C. Lippens, A.J. Burggrasst and P.L. Gellings, *J. Chem. Soc. Faraday Trans. 1* 83, 1485 (1987).
3. R. Vassen, X. Cao, F. Tietz, D. Basu and D. Stover, *J. Am. Ceram. Soc.* 8, 2023 (2000).
4. K.E. Sickafus, L. Minervine, R.W. Grimes, J.A. Valdez, M. Ishimaru, F. Li, K. J. McClellan and T. Hartmann, *Science* 289 748 (2000).
5. Gady W. G. Piezoelectricity Newyork; Dover (1964).
6. Caracoche M. C., Martinez J. A., Rivas P.C., International conference of advanced materials (2009).
7. Martinez J. A. *et al.*, XVII Latin American symposium on solid state physics, 242(9), 1838-1841 (2005).
8. Matsuhira K. *et al.*, *J. of Phys.*, 145(1), 012031 (2009).
9. Purushothama K.M., Shivarudraiah, Jebaraj P. M., *Int. J. Eng. Sci. And Tech.*, 3(3), 2236-2243 (2011).
10. M. Cusack, The electrical and magnetic properties of solids (London: Longmans) (1967).
11. J.P. Suchet, Electrical conduction in solids materials (London Pergamon) (1975).
12. L. F. Bates: Modern Magnetism London: Cambridge (1951).
13. A.N. Thakur, K. Gaur, M. A. Khan, and H.B. Lal, Magnetic study of gadolinium-iron-transition metal mixed oxides, *Ind. J. Phys.*, 71A (1), 91-97 (1997).

14. C. Kittel, Introduction to solid state physics, 7th edition John Wiley & Sons, Inc. (1996).
15. A.N. Thakur, K. Gaur and H.B. Lal, *Ind. J. Phys.* 70A(2), 225 (1996).
16. V. P. Srivastava, PhD. Thesis (University of Gorakhpur, India) (1998).
17. Nanda M.L. Goswami, Choudhary R.N.P., Mahapatra P. K., *Int. J. Phys.* 73A(4), 445-451 (1999).
18. Singh N.K., Sharma Seema, Choudhary R. N. P., *Ind. J. Phys.*, 74(1), 63-66 (2000).
19. Dekker A.J., *Solid State Physics*, Mac Millan, London, (1964).
20. A. N. Thakur, K. Gaur, M. A. Khan, and H.B. Lal, Magnetic study of gadolinium-iron-transition metal mixed oxides, *Ind. J. Phys.*, 71A (1), 91-97 (1997).